Clinical, Cosmetic and Investigational Dermatology

Dovepress
Taylor & Francis Group

Open Access Full Text Article

ORIGINAL RESEARCH

Mendelian Randomization and Experimental Validation Identify Key Immune Signatures in Bullous Pemphigoid

Zhimin Wang[1,2,*], Huan Cui[1,*], Lingzhi Meng[1], Xuesong Yang[3], Jianzhou Ye[3]

[1]First School of Clinical Medicine, Yunnan University of Traditional Chinese Medicine, Kunming, Yunnan, People's Republic of China; [2]Yunnan Key Laboratory of Southern Medicinal Utilization, Yunnan University of Chinese Medicine, Kunming, Yunnan, People's Republic of China; [3]Department of Dermatology, First Affiliated Hospital of Yunnan Traditional Chinese Medicine University, Kunming, Yunnan, People's Republic of China

*These authors contributed equally to this work

Correspondence: Xuesong Yang; Jianzhou Ye, Email yangxuesong@ynucm.edu.cn; yejianzhou@ynucm.edu.cn

Clinical, Cosmetic and Investigational Dermatology downloaded from https://www.dovepress.com/
For personal use only.

Objective: This study aims to investigate the potential causal relationships between genetically determined peripheral immunophenotypes and bullous pemphigoid (BP).

Methods: Leveraging publicly available genetic data from GWAS of 731 immunophenotypes and BP, we assessed potential associations between immunophenotypes and BP risk using Mendelian randomization (MR) and scRNA-seq of eQTLs analysis. The IVW method with FDR-adjusted q-values was the primary tool for estimating causal effects, supplemented by MR-Egger, weighted mode, weighted median, and simple mode for further investigation. LOO analysis, MR-PRESSO, and MR pleiotropy residual sum were used to ensure result robustness, exclude horizontal pleiotropy outliers, and assess heterogeneity. Single-cell sequencing data were used to explore transcriptional correlates of the MR-identified signatures, and flow cytometry was used to examine their changes in the circulation of BP-like mice.

Results: Two-sample MR identified 52 potential immune-related phenotypes associated with BP, of which monocyte-related signatures remained significant after false discovery rate (FDR) correction. Monocytic myeloid-derived suppressor cells (M-MDSCs), CD16 (FcγRIII) on CD14-CD16 + monocytes, and CD62L on monocytes were identified as having a potential causal association with BP, (M-MDSCs: OR=1.69, 95% CI=1.35–2.13, q=0.002; CD16: OR=0.83, 95% CI =0.75–0.92, q=0.038; CD62L: OR=0.53, 95% CI=0.39–0.72, q=0.011). scRNA-seq revealed that CD16 and CD62L expression was significantly upregulated in neutrophils and dendritic cells of BP patients; furthermore, Functional enrichment analysis showed these immune cells are involved in pathogen recognition and inflammatory response. In BP-like mice, flow cytometry detected an increase in M-MDSCs and a decrease in CD16 (FcγRIII) on CD14−CD16+ monocytes in the circulation; CD62L was not assessed in the murine model.

Conclusion: These findings suggest that M-MDSC absolute count is positively associated with BP risk, while CD62L expression on monocytes and CD16 expression on CD14−CD16+ monocytes are negatively associated. These immune signatures are potential contributors to BP susceptibility that require further mechanistic validation. However, the BP case cohort included in the GWAS dataset had a limited sample size; future mechanistic studies are needed to elucidate their specific underlying functional mechanisms.

Keywords: bullous pemphigoid, M-MDSCs, monocyte, MR analysis, CD16

Introduction

Bullous pemphigoid (BP), a potentially debilitating autoimmune subepidermal blistering disorder, is immunopathologically defined by autoantibodies directed against the hemidesmosomal antigens BP180 (COL17) and BP230. Tension blisters, pruritus rashes, and ulcers in the skin and mucosa characterize the condition. The cumulative incidence of BP has been estimated to be 8.2% per million population, while the incidence rate is 34.2% per million population per year.[1] The pathogenesis of BP involves various immune cells and factors, including T cells,[2] B cells,[3] complement cells,[4] mast cells,[5] neutrophils,[6] DC,[7] eosinophils,[8] and Epitope Spreading.[9] The complex etiopathogenesis of BP involves largely

https://doi.org/10.2147/CCID.S617562
Received: 26 April 2026
Accepted: 10 July 2026
Published: 21 July 2026

© 2026 Wang et al. This work is published and licensed by Dove Medical Press Limited. The full terms of this license are available at https://www.dovepress.com/terms.php and incorporate the Creative Commons Attribution – Non Commercial (unported, v4.0) License (http://creativecommons.org/licenses/by-nc/4.0/). By accessing the work you hereby accept the Terms. Non-commercial uses of the work are permitted without any further permission from Dove Medical Press Limited, provided the work is properly attributed. For permission for commercial use of this work, please see paragraphs 4.2 and 5 of our Terms (https://www.dovepress.com/terms.php).

unknown environmental and polygenic genetic risk elements. Local or systemic corticosteroids are considered the primary approach for treating BP; however, 40% of BP patients experience relapse during steroid tapering and require re-administration of corticosteroids or related immunosuppressive drugs.[3] The causal effect between immune cells and BP remains unclear. Although there is a considerable infiltration of immune cells in BP, the specific phenotypes of immune cells with a direct causal relationship with the pathogenesis of BP largely remain to be adequately investigated.

MR is a method of inferring exposure and outcome causality using genetic variants as instrumental variables (IVs). As genetic variants are single nucleotide polymorphisms (SNPs) independent of confounding factors or reverse causality,[10] randomized controlled experiments, in comparison to MR designs, have limitations such as ethical constraints, selection bias, the requirement for large sample sizes, limited generalizability to practical applications, and substantial time and resource consumption.

Single-cell sequencing[11] allows for the accurate identification of cellular heterogeneity in diseases; however, its limitations include high cost, challenging sample processing, and technical noise leading to cell damage, RNA loss, and potential generation of false positive or false negative results during the sequencing process pose significant challenges. Natural random allocation[12,13] can help eliminate confounding factors in observational studies and assist in establishing causal direction; this approach also prevents reverse causality. Moreover, it reduces selection bias, information bias, recall bias, and other issues inherent in observational research, thus enhancing the internal validity of study findings.

Although previous studies have revealed the roles of various immune cells in the pathogenesis of BP, there is still a lack of systematic research on the causal relationship between immune cells and BP. Mendelian randomization, as a powerful method for causal inference, combined with the precise analysis of cellular heterogeneity by single-cell sequencing technology, provides new ideas and approaches for us to deeply explore the immune mechanisms of BP. To address this knowledge gap, we undertook a comprehensive study that synergizes the causal inference power of Mendelian randomization with the high-resolution cellular profiling of single-cell RNA sequencing. Furthermore, flow cytometry was used to verify our findings in the peripheral blood samples of BP-like mice. This integrative approach allows us to not only identify putative causal immune cell phenotypes but also to delineate their molecular signatures within the BP tissue microenvironment.

Materials and Methods

Exposure and Outcome Data Sources

Our two-sample MR framework was implemented using summary statistics from distinct, publicly available GWAS. The exposure data comprised 731 immunophenotypes from the GWAS Catalog (GCST90001391 to GCST90002121),[14] quantifying immune features such as absolute and relative cell counts, surface antigen abundance, and cellular morphology across B cell, dendritic cell, T cell, monocyte, myeloid, and TBNK panels. This foundational GWAS was performed in a non-overlapping cohort of 3757 European participants. Genetic associations for the outcome, BP, were obtained from the FinnGen Biobank (IEU OpenGWAS project; finn-b-L12_PEMPHIGOID_BULL), comprising 219 cases and 218,066 controls of European descent. Furthermore, we leveraged a publicly available single-cell RNA-seq dataset (GEO; Zenodo: 10924853) from Tingting Liu et al,[15] profiling PBMCs from 8 BP patients and 8 healthy controls, to provide transcriptional validation of our genetically inferred findings at the cellular level An overview of this analytical design is depicted in Figure 1.

Genetic Instrumental Variable Selection

For the blood cell traits derived from the GWAS datasets, genetic variants achieving genome-wide significance were selected at the p-value cutoff of 5×10^{-8}($p < 5\times10-8$). In order to obtain independent IVs, clumping ($R^2 < 0.001$ within a 10,000-kb distance) was performed based on the linkage disequilibrium (LD) reference panel of the 1000 Genomes Project. Additionally, to avoid bias from weak instruments, we considered IVs with F statistics >10 as robust instruments and reserved them for the following analysis. The exposure and outcome SNPs were harmonized to ensure that effect estimates were aligned for the same effect allele. Palindromic SNPs with intermediate effect allele frequencies (EAFs > 0.42) or SNPs with incompatible alleles were discarded.[16]

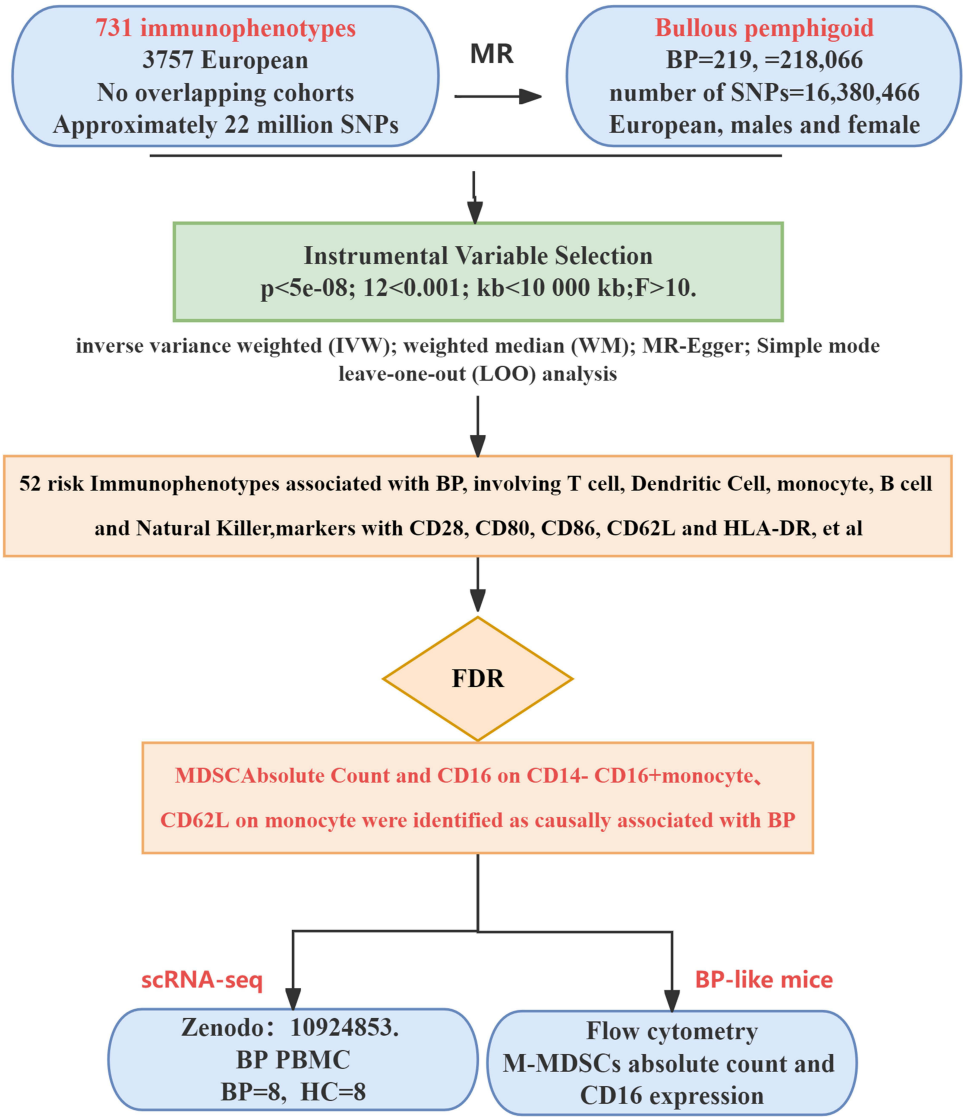

Figure 1 Overview of the overall design and process of the study. Blue rounded rectangles: Red text highlights Summary statistics sources for exposure (731 immunophenotypes) and outcome (BP). Diamond shape: Red text highlights the three monocyte-related immunophenotypes that remained statistically significant after FDR correction, prioritizing them for subsequent scRNA-seq and a BP-like mouse model validation. The bottom two branches represent follow-up experiments involving peripheral blood scRNA-seq and in vivo murine model validation to cross-verify the MR genetic findings.

Statistical Analyses

A comprehensive analytical pipeline was established in R (v3.5.3) to evaluate the putative causal effects of immunophenotypes on BP. Our primary causal estimates were derived from random-effects inverse variance weighted (IVW) and weighted median (WM) methods.[17] The robustness of these estimates was rigorously challenged through multiple sensitivity analyses: Heterogeneity was assessed with Cochran's Q statistic;[18] directional pleiotropy was tested via the MR-Egger intercept;[19,20] and the radial MR test and MR-PRESSO global test were implemented to identify and exclude pleiotropic outliers.[21,22] The stability of the results was further confirmed by leave-one-out sensitivity analysis. A two-tiered significance threshold was adopted, with FDR correction ($q < 0.05$) applied to primary IVW findings and a nominal $p < 0.05$ level for sensitivity tests.

Analysis Methods for Single-Cell Sequencing

The scRNA-seq dataset was processed and analyzed using a standardized workflow in Seurat. Following stringent cell-level QC (200 < nFeature_RNA < 10,000; mitochondrial ratio < 10%), the gene expression matrix was normalized and

https://doi.org/10.2147/CCID.S617562

scaled.[23,24] Dimensionality reduction was performed using PCA, followed by graph-based clustering to delineate distinct cell populations. The "FindMarkers" function enabled identification of differentially expressed genes between comparative groups. To extend our analysis beyond differential expression, we utilized the SCENIC algorithm[25] to reconstruct gene regulatory networks and infer transcription factor activity. The biological implications of the gene signatures were subsequently elucidated through functional enrichment analysis against the GO and KEGG databases.[26,27]

Circulatory Blood Flow Detection in BP-Like Mice

We induced a BP model in NC16A+/+ humanized transgenic mice by subcutaneous injection of anti-BP180 IgG antibodies (cumulative dose: 200 μg; 50 μg every other day). More experimental details can be found in the Supplementary Methods. At the end of the experiment, mice were euthanized by CO_2 inhalation followed by cervical dislocation in accordance with the AVMA Guidelines for the Euthanasia of Animals. Subsequently, flow cytometry was employed to analyze the proportion of specific cell populations in the mouse circulation. The experiment was approved by the Animal Ethics Committee of Yunnan Minzu University (YMU-AFEC-2023-A020). All flow cytometry antibodies were purchased from BioLegend, specifically including: APC anti-mouse CD16/32 (101,325), PE anti-mouse CD14 (150,105), FITC anti-mouse/human CD11b (101,205), PE/Cyanine5 anti-mouse Ly-6G/Ly-6C (Gr-1) (108,409). Data acquisition was performed using a C6 PLUS flow cytometer (BD Biosciences, USA), and imaging was conducted with a DM1000 microscope (Leica, Germany). Peripheral blood mononuclear cells (PBMC) were isolated from mice using density gradient centrifugation. After resuspension in 2% FBS-PBS and washing once by centrifugation at 1500 rpm for 5 min, the cell concentration was adjusted to 1×10^6 cells/100 μL, and 100 μL was aliquoted per flow tube. Following supernatant removal, APC-labeled anti-CD16 and PE-labeled anti-CD14 antibodies were added. The samples were vortexed to mix and incubated at room temperature for 15 min to perform extracellular staining; subsequently, 800μL of Cell Staining Buffer was added, and the cells were centrifuged at 1200 × g (calculated based on a radius of 3.5 cm) for 5 min. After discarding the supernatant, FITC-labeled anti-CD11b antibody and PE/Cyanine5-labeled anti-Gr-1 antibody were added and incubated at 4°C for 45 min to complete staining; finally, 500μL of Staining Buffer was added, and the samples were run on the machine. M-MDSCs were identified and their proportion calculated by gating on CD11b+Gr-1low; within the CD11b+Gr-1low monocyte gate, further gating was performed on CD14- to analyze the expression level of CD16/32 (CD16) in this subpopulation. Finally, the distribution of murine M-MDSCs and CD16 expression profiles within the CD14−CD16+ subpopulation were visualized using two-parameter dot plots.

Results

Investigating the Association Between Immunophenotypes on BP Using Mendelian Randomization

Two-sample MR analysis was performed to explore the causal effects of immunophenotypes on BP, and the IVW method was used as the primary analysis. The causal effect estimates of immunophenotypes on BP susceptibility were obtained after the selection and harmonization of IVs, as shown in Table 1 and Figure 2. At a significance level of 0.05, 52 distinct immune phenotypes were identified, with 20 observed on the T cell panel, 12 on the cDC panel, 10 on the monocyte panel, 5 on the B cell panel, 4 on the NK cell panel, and the final one, CX3CR1, on CD14-CD16-. The results of IVW analysis suggested a potential genetic association between a higher liability of BP and circulating T cell phenotype. The most significant ones were CD28-CD8dim T cell absolute count [odds ratio (OR) =0.30, 95% CI = 0.12–0.76, p=0.001]; CD45RA on naive CD8+T cells [IVW *OR* = 2.10, 95% CI = 1.32–3.32, *p* =0.002]; HVEM on naive CD8+T cells [IVW *OR* = 0.55, 95% CI = 0.36–0.83, *p* =0.005], followed by the dendritic cell phenotype, with CD62L-dendritic cell absolute count [IVW *OR* = 1.34, 95% CI = 1.09–1.66, *p* =0.006]. The monocyte phenotype was also significant with CD16 on CD14-CD16+monocytes [IVW *OR* = 0.83, 95% CI = 0.75–0.92, *p* =0.000]; M-MDSCs absolute count [IVW *OR* = 1.69, 95% CI = 1.35–2.13, *p* =0.000]; CD62L on monocytes [IVW *OR* = 0.53, 95% CI = 0.39–0.72, *p* =0.000]; CD16 +monocyte %monocyte [IVW *OR* = 0.58, 95% CI = 0.40–0.83, *p* =0.003]; CD64 on CD14-CD16+monocyte [IVW *OR* = 4.00, 95% CI = 1.78–8.98, *p* =0.001]. Although B cells exhibited only five phenotypes, four of them showed suggestive associations with BP, CD20 on IgD-CD24-B cells [IVW *OR* = 0.39, 95% CI = 0.21–0.70, *p* =0.002]; CD24 on memory

Table 1 The Causal Associations Between BP and Immune Cell Traits

	Immunophenotypes	MR method	n SNP	Beta	SE	OR (95% CI)	P	P for MR-Egger intercept	Q_pval (Heterogeneity)
1	CCR7 on naive CD4+ T cell	MR-IVW	6	0.379	0.178	2.07 (1.03–2.07)	0.034	0.415	0.695
2	CD4 on CD39+ CD4+ T cell	MR-IVW	29	−0.246	0.097	0.78 (0.65–0.95)	0.011	0.910	0.241
3	CD25 on CD39+ secreting CD4 regulatory T cell	MR-IVW	3	0.622	0.276	1.86 (1.08–3.20)	0.024	0.998	0.870
4	CD25 on secreting CD4 regulatory T cell	MR-IVW	3	0.589	0.26	1.80 (1.08–3.00)	0.023	0.962	0.897
5	CD28- CD4-CD8- T cell Absolute Count	MR-IVW	3	0.783	0.361	0.46 (0.23–0.93)	0.030	0.797	0.899
6	CD28- CD8+ T cell Absolute Count	MR-IVW	7	−0.601	0.238	0.55 (0.34–0.87)	0.012	0.645	0.596
7	CD28- CD8dim T cell Absolute Count	MR-IVW	3	−1.216	0.374	0.30 (0.12–0.76)	0.001	0.778	0.924
8	CD28- CD8dim T cell %T cell	MR-IVW	5	−0.747	0.306	0.47 (0.26–0.86)	0.015	0.135	0.365
9	CD28 on CD28+ CD45RA+ CD8+ T cell	MR-IVW	9	0.403	0.16	1.50 (1.09–2.05)	0.012	0.454	0.970
10	CD39+ CD8+ T cell %CD8+ T cell	MR-IVW	111	−0.094	0.048	0.91 (0.83–1.00)	0.048	0.213	0.532
11	CD39 on CD39+ CD8+ T cell	MR-IVW	12	−0.373	0.17	0.69 (0.49–0.96)	0.029	0.927	0.511
12	CD45RA- CD4+ T cell Absolute Count	MR-IVW	3	−0.571	0.264	0.56 (0.34–0.95)	0.030	0.792	0.891
13	CD45RA on naive CD8+ T cell	MR-IVW	7	0.74	0.235	2.10 (1.32–3.32)	0.002	0.739	0.671
14	Effector Memory CD4+ T cell Absolute Count	MR-IVW	2	−0.643	0.308	0.53 (0.29–0.96)	0.037	NA	0.737
15	HLA DR+ CD8+ T cell Absolute Count	MR-IVW	11	−0.395	0.166	0.67 (0.49–0.93)	0.017	0.662	0.533
16	HLA DR+ CD8+ T cell %lymphocyte	MR-IVW	9	−0.425	0.212	0.65 (0.12–1.02)	0.045	0.234	0.199
17	HLA DR+ CD8+ T cell %T cell	MR-IVW	10	−0.401	0.2	0.67 (0.45–0.99)	0.045	0.353	0.244
18	HLA DR+ T cell%lymphocyte	MR-IVW	13	−0.361	0.157	0.70 (0.51–0.95)	0.022	0.77	0.476
19	HLA DR+ T cell%T cell	MR-IVW	12	0.343	0.159	0.71 (0.52–0.97)	0.031	0.992	0.486
20	HVEM on naive CD8+ T cell	MR-IVW	6	−0.606	0.214	0.55 (0.36–0.83)	0.005	0.598	0.626
21	CD62L- CD86+ mDC Absolute Count	MR-IVW	36	0.16	0.077	1.17 (1.01–1.36)	0.037	0.959	0.358
22	CD62L- CD86+ mDC % Dendritic Cell	MR-IVW	36	0.172	0.081	1.19 (1.01–1.39)	0.034	0.932	0.183
23	CD62L- Dendritic Cell Absolute Count	MR-IVW	24	0.295	0.107	1.34 (1.09–1.66)	0.006	0.658	0.423
24	CD80 on CD62L+ myeloid Dendritic Cell	MR-IVW	6	0.466	0.235	1.59 (1.01–2.52)	0.047	0.222	0.704
25	CD80 on myeloid Dendritic Cell	MR-IVW	8	0.474	0.205	1.61 (1.07–2.40)	0.021	0.772	0.443
26	CD86+ myeloid Dendritic Cell Absolute Count	MR-IVW	26	0.194	0.092	1.20 (1.01–1.45)	0.035	0.756	0.365
27	CD86+ myeloid Dendritic Cell %Dendritic Cell	MR-IVW	25	0.2	0.094	1.22 (1.02–1.47)	0.033	0.608	0.316
28	CD86 on myeloid Dendritic Cell	MR-IVW	7	0.482	0.222	1.62 (1.05–2.50)	0.030	0.995	0.282
29	Dendritic Cell Absolute Count	MR-IVW	15	0.048	0.174	1.62 (1.15–2.28)	0.006	0.993	0.197
30	HLA DR on myeloid Dendritic Cell	MR-IVW	86	−0.16	0.061	0.85 (0.76–0.96)	0.009	0.794	0.00E+00
31	Myeloid Dendritic Cell Absolute Count	MR-IVW	18	0.353	0.146	1.42 (1.07–1.89)	0.015	0.88	0.150
32	Myeloid Dendritic Cell %Dendritic Cell	MR-IVW	15	0.353	0.178	1.42 (1.00–2.02)	0.048	0.768	0.091
33	CD14+ CD16+ monocyte Absolute Count	MR-IVW	19	−0.338	0.134	0.71 (0.55–0.93)	0.012	0.661	0.210
34	CD14+ CD16- monocyte %monocyte	MR-IVW	8	0.496	0.194	1.64 (1.12–2.40)	0.011	0.453	0.729
35	CD16+ monocyte %monocyte	MR-IVW	10	−0.547	0.183	0.58 (0.40–0.83)	0.003	0.576	0.850

(*Continued*)

https://doi.org/10.2147/CCID.S617562

Table 1 (Continued).

	Immunophenotypes	MR method	n SNP	Beta	SE	OR (95% CI)	P	P for MR-Egger intercept	Q_pval (Heterogeneity)
36	CD16 on CD4+ CD16+ monocyte	MR-IVW	30	−0.192	0.09	0.83 (0.69–0.98)	0.032	0.925	0.436
37	CD16 on CD14- CD16+ monocyte	MR-IVW	79	−0.191	0.052	0.83 (0.75–0.92)	0.000	NA	0.436
38	CD62L on monocyte	MR-IVW	9	−0.628	0.155	0.53 (0.39–0.72)	0.000	0.175	0.430
39	CD64 on CD14- CD16+ monocyte	MR-IVW	4	1.385	0.413	4.00 (1.78–8.98)	0.001	0.373	0.648
40	M-MDSCsAbsolute Count	MR-IVW	18	0.528	0.116	1.69 (1.35–2.13)	0.000	0.198	0.096
41	PDL-1 on CD14- CD16+ monocyte	MR-IVW	11	−0.275	0.138	0.76 (0.58–0.99)	0.046	0.594	0.717
42	SSC-A on CD14+ monocyte	MR-IVW	27	0.228	0.094	1.26 (1.05–1.51)	0.015	0.963	0.487
43	CD20 on IgD- CD24- B cell	MR-IVW	4	−0.951	0.303	0.39 (0.21–0.70)	0.002	0.678	0.134
44	CD24 on IgD- CD38- B cell	MR-IVW	5	0.434	0.098	1.54 (1.05–2.27)	0.028	0.663	0.778
45	CD24 on memory B cell	MR-IVW	8	0.542	0.191	1.72 (1.18–2.50)	0.004	0.645	0.882
46	HLA DR on B cell	MR-IVW	39	0.363	0.114	1.44 (1.15–1.80)	0.001	0.202	0.00E+00
47	IgD on IgD+ CD24+ B cell	MR-IVW	28	0.294	0.105	1.34 (1.09–1.65)	0.005	0.122	0.489
48	HLA DR+ Natural Killer %Natural Killer	MR-IVW	24	−0.25	0.116	0.78 (0.62–0.98)	0.031	0.701	0.187
49	HLA DR on HLA DR+ Natural Killer	MR-IVW	29	−0.303	0.14	0.74 (0.56–0.97)	0.031	0.691	0.00E+00
50	Natural Killer Absolute Count	MR-IVW	3	0.77	0.369	2.16 (1.05–4.45)	0.037	0.605	0.731
51	SSC-A on HLA DR+ Natural Killer	MR-IVW	17	−0.25	0.126	0.78 (0.61–1.00)	0.047	0.487	0.719
52	CX3CR1 on CD14- CD16-	MR-IVW	14	0.372	0.16	1.45 (1.06–1.99)	0.020	0.635	0.814

Note: IVW, inverse variance weighting, primarily listing the IVW results before FDR correction.

https://doi.org/10.2147/CCID.S617562

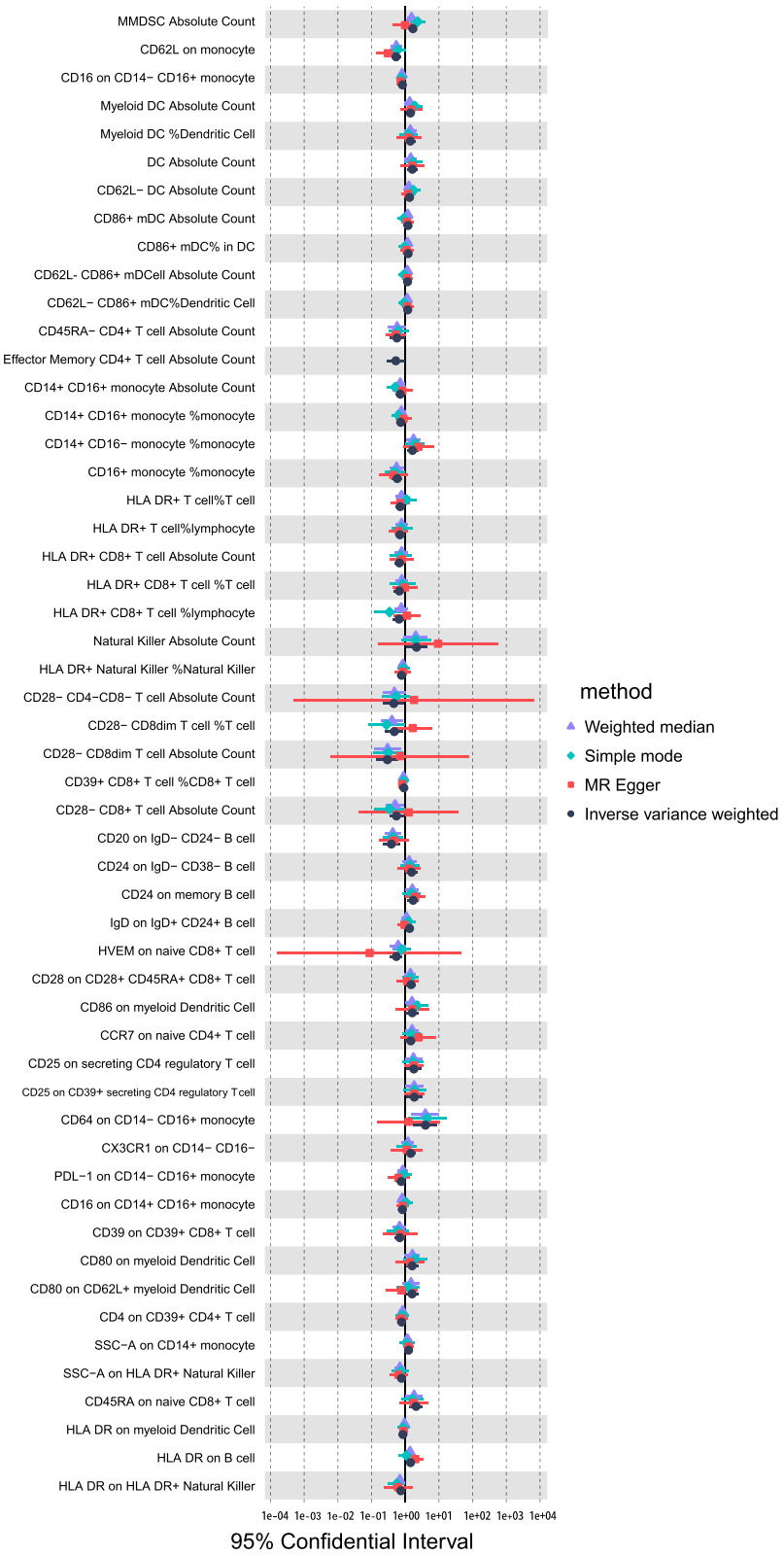

Figure 2 Forest plot for the causal effect of circulating immune cells on the risk of BP derived from inverse variance weighted (IVW), MR Egger weighted median, and simple mode (before FDR).
Abbreviations: OR, odds ratio; CI, confidence interval.

https://doi.org/10.2147/CCID.S617562

B cells [IVW *OR* = 1.72, 95% CI = 1.18–2.50, *p* =0.004]; HLA DR on B cells [IVW *OR* = 1.44, 95% CI = 1.15–1.80, *p* =0.001]; IgD on IgD+CD24+B cells [IVW *OR* = 1.34, 95% CI = 1.09–1.65, *p* =0.005]. Lastly, we focused on NK cells and CX3CR1 on CD14-CD16-. Sensitivity analysis using the "leave-one-out" method indicated that no single SNP disproportionately influenced the estimates (Table 1).

As showed in Figure 3. After performing FDR correction, the remaining significant associations included the absolute count of M-MDSCs (q-value = 0.002), which was identified as a potential risk factor, while CD62L on monocytes (q-value = 0.011) and CD16 on CD14-CD16+ monocytes (q-value = 0.038) were suggested as potential protective factors. These markers represent the most strongly associated immunophenotypes with BP in the present MR analysis. A notable feature was that all these associations manifested explicitly in the monocyte panel.

Identification of Differentially Expressed Genes Using Single-Cell Sequencing Analysis

To explore whether the coding genes of 3 circulating cell types had any cell type-specific enrichment in BP, we further performed single-cell type expression analysis using single-cell RNA-seq data. Initial screening was performed to eliminate low-quality data. Following this, cell clustering was conducted using the FindNeighbors and FindClusters functions, identifying 15 distinct cellular populations (B cells, DC, Effector CD8 T, MAIT cells, Megakaryocytes, Memory CD4 T, Monocytes, Naive CD4 T, Naive CD8 T, Neutrophils, NK-1, NK-2, pDC, Proliferating T, unknown) (Figure 4A). We used heatmaps to visualize the expression of FCGR3A (CD16), SELL (CD62L), CD28, HLA-DRA, and HLA-DRB1 across different cell populations. It can be seen that FCGR3A (CD16) is mainly expressed in Neutrophils and NK-1 cells, SELL (CD62L) is mainly concentrated in Megakaryocytes, Memory CD4 T cells, Monocytes, and B cells, while CD28 is expressed in all other cell subsets to varying degrees except B cells and NK-1 cells. Finally, HLA-DRA and HLA-DRB1 were predominantly expressed in B cells, DC cells, and Monocytes (Figure 4B). The dot plot reveals that in BP patients, CD16 and CD62L expression was significantly elevated on neutrophils (whereas in the HC group, significant expression was observed only on NK and T cells); HLA-DRA and HLA-DRB1 were significantly upregulated on DCs, while alterations in CD28 were primarily observed in T cell subsets, mirroring the trends shown in the heatmap (Figure 4C, Red box). Using the Seurat package's VlnPlot function, we generated violin plots of marker

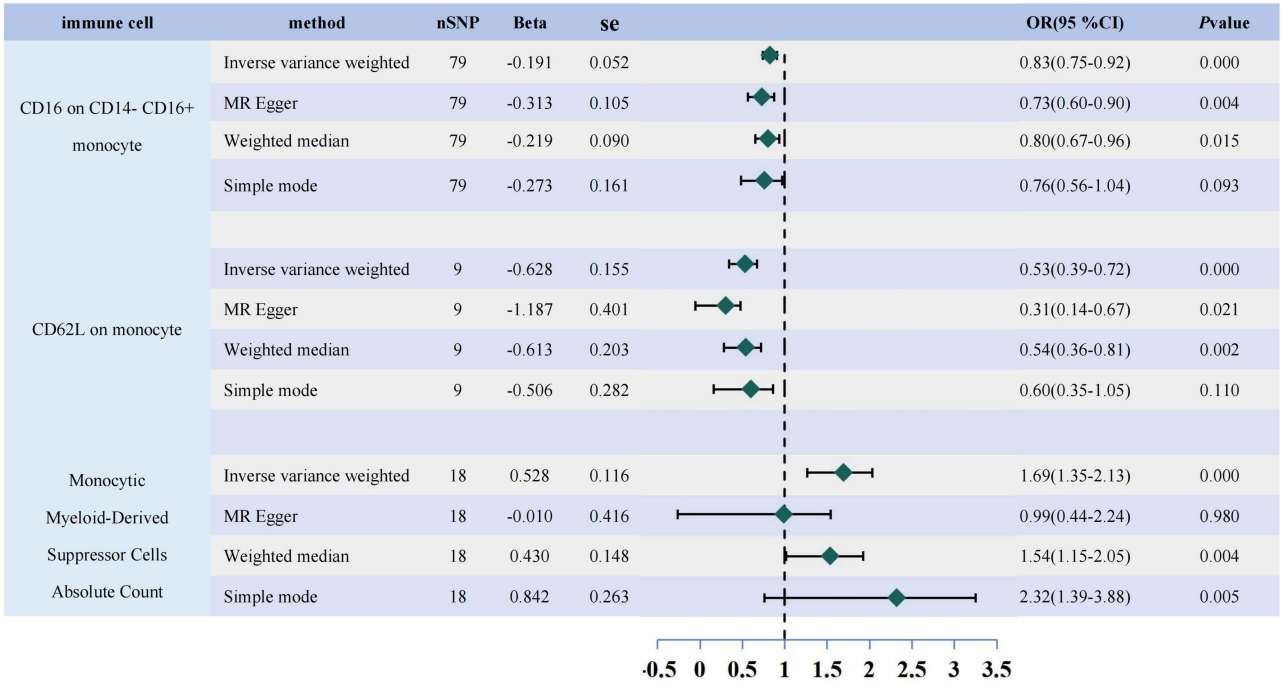

Figure 3 Forest plot for the causal effect of circulating immune cells on the risk of BP derived from inverse variance weighted (IVW), MR Egger weighted median, and simple mode (after FDR).
Abbreviations: OR, odds ratio; CI, confidence interval.

https://doi.org/10.2147/CCID.S617562

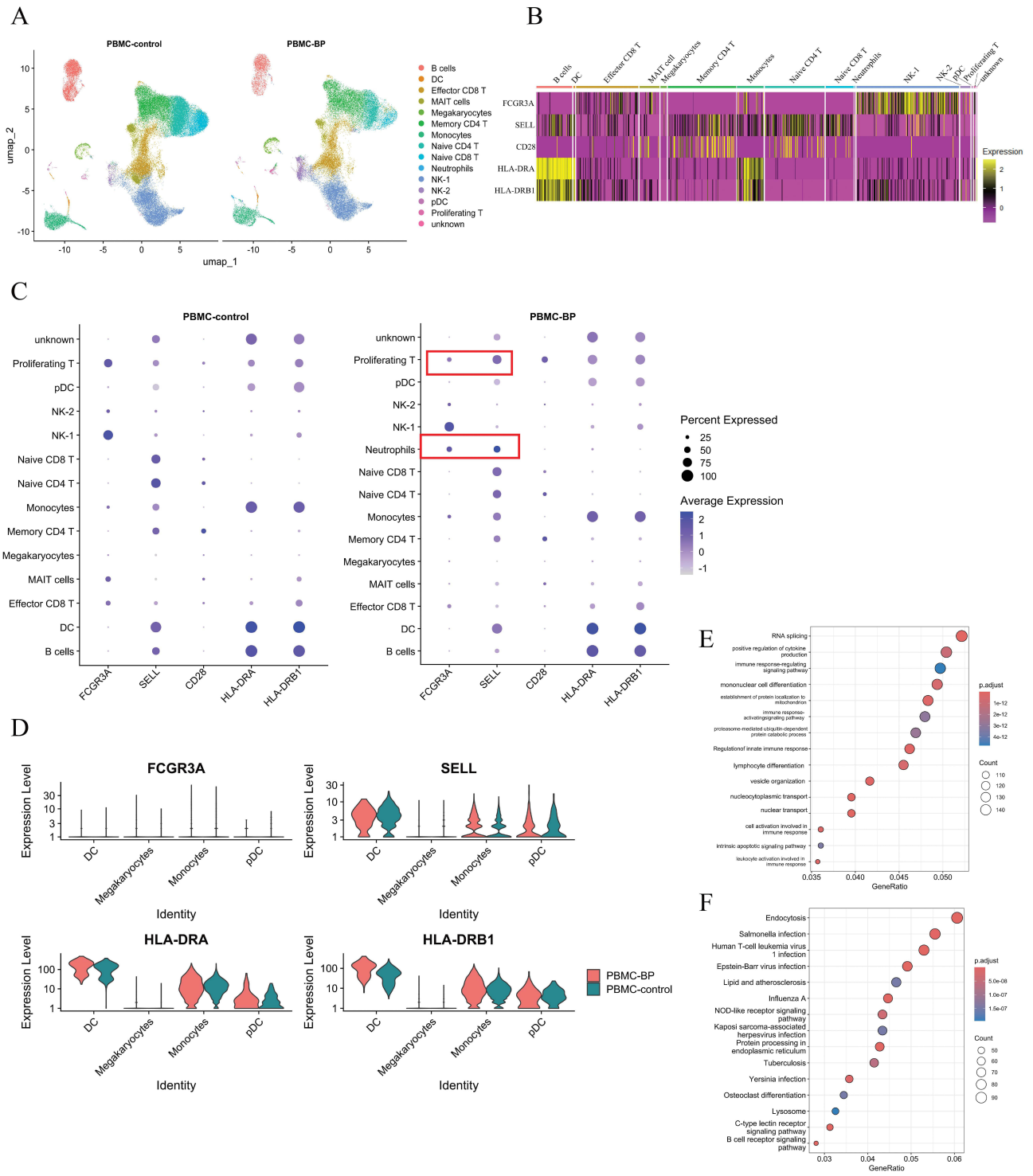

Figure 4 Analysis of scRNA-seq data of circulating immune cells in patients with BP. (**A**) UMAP plot of cell subpopulations in BP and HC. (**B**) Heatmap depicting the expression levels of FCGR3A (CD16), SELL (CD62L), CD28, HLA-DRA, and HLA-DRB1 across various cell subpopulations. (**C**) Dot plot comparing cell type-specific gene expression between BP patients and healthy controls. (**D**) Violin plot of gene expression of FCGR3A (CD16), SELL (CD62L), CD28, HLA-DRA, and HLA-DRB1 in monocyte subpopulations. (**E**) Gene Ontology (GO) enrichment analysis of monocyte-related genes. (**F**) Kyoto Encyclopedia of Genes and Genomes (KEGG) pathway enrichment analysis of monocyte-related genes. Red rectangular boxes indicate the target cells.

https://doi.org/10.2147/CCID.S617562

gene expression, including FCGR3A (CD16), SELL (CD62L), CD28, HLA-DRA and HLA-DRB1, demonstrating their distribution across monocyte subpopulations. The results showed that FCGR3A (CD16) was minimally expressed, and SELL (CD62L) was marginally elevated in monocytes compared with the HC group, but the difference was not significant (Figure 4D). Conducting GO enrichment analysis on monocyte genes revealed their significant involvement in immune-related processes, such as RNA splicing, positive regulation of cytokine production, immune response-regulating signaling pathway and mononuclear cell differentiation (Figure 4E). KEGG enrichment analysis identified the NOD-like receptor signaling pathway, the C-type lectin receptor signaling pathway, and the B cell receptor signaling pathway (Figure 4F).

Levels of M-MDSCs and CD14-CD16+Monocytes in Peripheral Circulation of BP-Like Mice

After injection of anti-BP180 antibodies, erythema and minor ulcerations appeared on the dorsal skin of the mice (Figure 5A). HE staining revealed dermal-epidermal separation (Figure 5B, Blue arrows), and immunofluorescence showed linear deposition of C3 and IgG at the basement membrane zone (Figure 5C, Blue arrows). Flow cytometry results indicated a significant increase in the proportion of M-MDSCs in the peripheral blood of BP mice ($P<0.0001$) (Figure 5D and E). Even before the injection of anti-BP180 antibodies, this proportion showed a changing trend, but the difference was not statistically significant ($P=0.06$). Flow cytometry results also showed an increase in the CD16 on CD14- CD16+ monocytes population in NC16A+/+ humanized transgenic mice, and after injection of anti-BP180 antibodies, the proportion of this cell population significantly decreased ($P=0.0047<0.01$)(Figure 5D and F).

Discussion

Globally, BP is a rare autoimmune blistering skin disease characterized by a substantial disease burden, frequent recurrence, and significant mortality. This condition predominantly affects the elderly population. The pathogenesis of BP involves antigen-presenting cells presenting antigens to reactive T cells, thereby activating them. This activation stimulates B cell maturation into plasma cells, which produce autoantibodies targeting the BP180 and BP230 structural proteins, ultimately resulting in subepidermal blister formation.[28] There are numerous immunological studies on BP, and most of them acknowledge that a combination of genetic predisposing factors, such as class II HLA,[29] and environmental influences, such as exposure to UV radiation and drugs, may contribute to the loss of immune tolerance toward antigens located at the dermal-epidermal junction.[30] It has also been proposed that this occurs due to an equilibrium disruption between autoreactive T helper (Th) cells and T regulatory (Treg) cells.[31,32] Activated DC trigger type 2 inflammatory responses in BP.[7] These studies largely focus on immune dysregulation and predictive indicators after BP onset, making it difficult to establish the temporal sequence and causal direction between immune cells or immune factors and the disease. Our study aimed to evaluate the genetic correlations and causal relationships between the immune cell and BP. Based on our results before the correction, 52 distinct immune phenotypes were identified, with 20 observed on the T cell panel, 12 on the cDC panel, 10 on the monocyte panel, 5 on the B cell panel, 4 on the NK cell panel, and the final one, CX3CR1, on CD14-CD16-. Our IVW analysis results suggested a potential genetic association between an increased genetic liability to BP and a circulating T cell phenotype, which is consistent with research categorizing BP as a type 2 immune reaction disorder.[2,33] T-cell activation by an autoantibody molecule can induce various responses, leading to the differentiation of B cells into plasma cells that secrete autoantibody β. Some of these plasma cells can produce IgM and IgG autoantibodies against COL17 and BP230[2,34] subsequently producing autoantibodies associated with BP. One distinctive feature of our results was that irrespective of the immune cell type, CD25, CD28, CD80, CD86, and HLA-DR expression showed genetic associations with BP in MR analysis. Rituximab primarily alleviated BP symptoms by targeting the CD20 surface protein expressed on B lymphocytes.[35] RTX achieves B-cell depletion through multiple pathways, thereby reducing the production of pathogenic antibodies. IgD- CD24- B cells, characterized as mature plasma cells, secrete pathogenic antibodies and express CD20 minimally. CD20 serves as the primary target for B-cell depletion. According to our research findings, CD20 expression on IgD- CD24- B cells is negatively correlated with BP ($b=-0.951$), which may provide additional insights into the causal relationship between CD20 on IgD- CD24- B cells and BP. These MR results suggest a genetic association

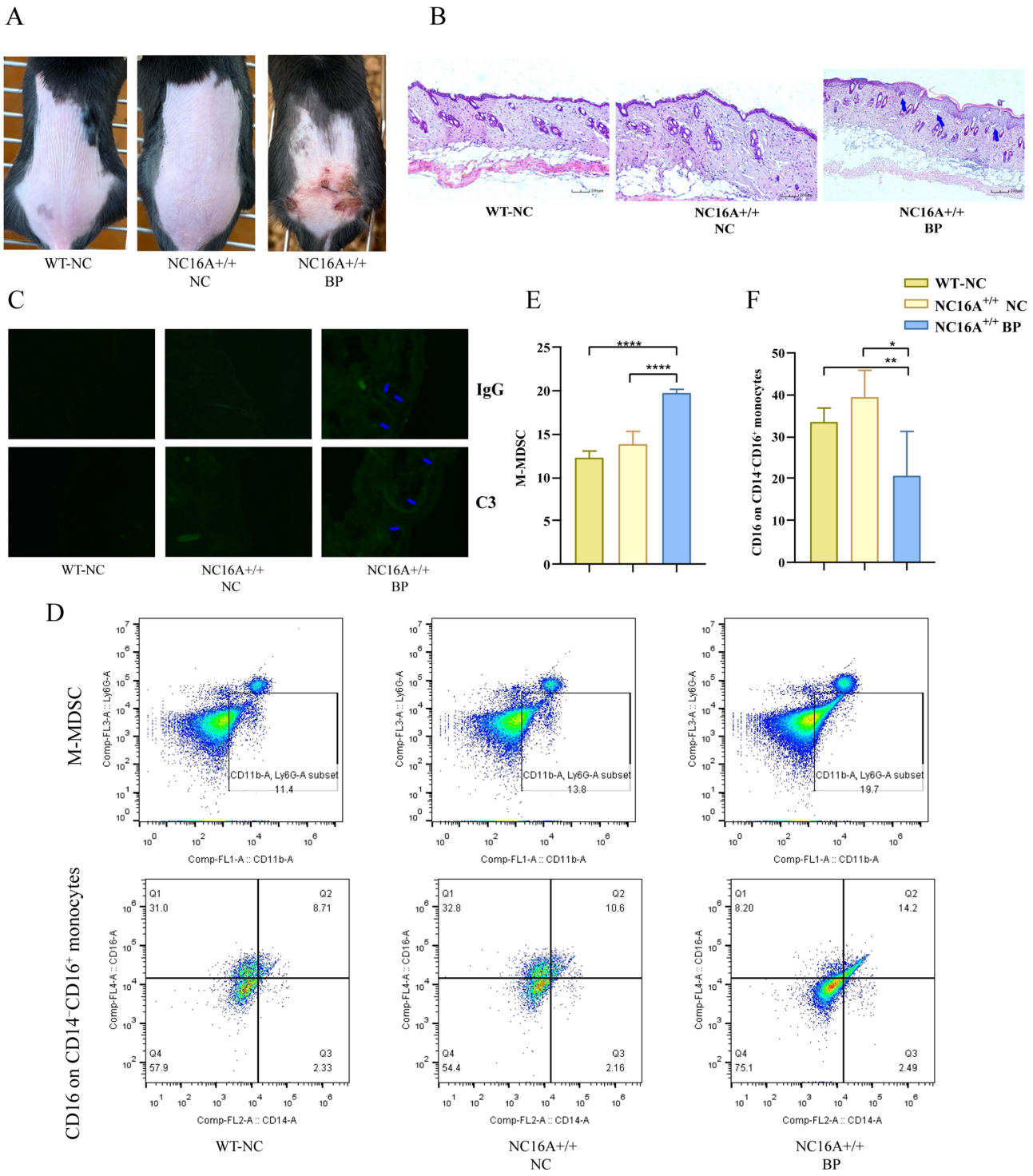

Figure 5 Alterations in the frequencies of M-MDSCs and CD14-CD16+ monocytes in the peripheral circulation of BP-like mice. (**A**) Appearance of the dorsal skin of mice; (**B**) HE staining of skin tissue; (**C**) Direct immunofluorescence staining of skin tissue; (**D**) Flow cytometric analysis of the proportions of M-MDSCs and CD14-CD16+ monocytes in peripheral blood; (**E**) Quantification of M-MDSC proportions; (**F**) Quantification of CD14-CD16+ monocytes proportions. Blue arrows point to the key lesions.* indicates P <0.05, ** indicates P <0.01, **** indicates P <0.0001 (n=5).

https://doi.org/10.2147/CCID.S617562

between reduced CD20 expression on IgD- CD24- B cells and increased BP risk; however, whether this reflects a causal biological mechanism requires further investigation.

According to our results, CD28 expression was genetically associated with BP in our MR analysis, suggesting a potential role in BP pathogenesis. CTLA-4 shares a high degree of homology, approximately 70%, with CD28. CTLA-4 and CD28 bind to the same ligands, CD80 and CD86, which serve as co-stimulatory signals for T cell activation. Our results indicate that the immunophenotype of immune cells lacking CD28 is negatively correlated with BP. Furthermore, scRNA-seq analysis supports that in the context of BP, CD28 alterations are primarily observed in the T cell panel, while the expression of CD80 and CD86 had a positive causal relationship with BP, implying that a higher abundance of CD28-negative T cells correlates with increased expression of CD80 and CD86 on DCs, thereby elevating the risk of BP. It is possible that under the CD28 deficiency, the transendocytosis mediated by CTLA-4 no longer utilizes rapid internalization and recycling of CTLA-4 to limit the binding of ligands (CD80, CD86) to CD28, resulting in a malfunction in the cycling of CTLA-4,[36] potentially contributing to BP pathogenesis, though this mechanistic hypothesis requires experimental validation. A review article[37] on the cutaneous toxicity of immune checkpoint inhibitors revealed that ipilimumab (targeting CTLA-4) can induce BP within two weeks of anticancer treatment. Following treatment, patients develop blisters that contain either serous or hemorrhagic fluid. This medication swiftly triggers the lysosomal degradation of cell-surface CTLA-4, thereby disrupting its normal cycling, which may be attributed to a reduction in CD4+, CD25+, and Foxp3+ regulatory T cells. The decline in T regulatory cells could facilitate the expansion of autoantibody-producing B cell clones that target antigens present in the basement membrane of the skin. Additionally, the reduction of CD28 protein diminishes T cell reactivity to external stimuli, indicating a potential link between CD28 deficiency and compromised T cell functionality. Consequently, T cells that lack CD28 can be classified as a subset of exhausted T cells.[38] CD28 deficiency also indirectly affects B cells, leading to defective development of follicular helper T cells, resulting in a lack of high-affinity, class-switched antibodies, and, consequently, T cell helper dysfunction,[39,40] which induces memory B cells to secrete IgG and IgE. Therefore, CD28 stimulation may be crucial in BP immunity, and blocking CD28 co-stimulation could serve as an immunosuppressive therapeutic approach for BP.

HLA-DR is a primary subtype of MHC-class molecules and a key member involved in specific recognition and antigen presentation in the body. It is typically expressed as a marker of activated T cells, as it remains unexpressed during quiescence. The inverse causal relationship between T cell-specific HLA-DR expression and BP risk in our preliminary analysis points toward a protective mechanism. This genetic inference is substantiated by immunological studies across diverse populations. Research on Caucasian patients suggests that specific HLA-DRB1 alleles may act as a protective haplotype by tempering the autoimmune attack on DEJ antigen.[41,42] Collectively, these studies suggest that HLA-DRB1 molecules may exert a regulatory role in the autoimmune response to BP antigens. Additionally, László S et al[43] found a significant correlation between the frequency of HLA-DR, high cell population and disease activity in BP, indicating a potential protective role in the pathogenesis of BP in northern China.[44] The above studies are relatively consistent with our findings.

The most noteworthy findings of the present study include the identification of three immunophenotypes, all residing within the mononuclear cell panel, following our FDR correction. These include the absolute count of M-MDSCs (OR=1.69, q=0.002), identified as a risk factor, whereas CD62L expression on monocytes (OR=0.53, q=0.011) and CD16 on CD14- CD16+ monocytes (OR=0.83, q=0.038) were identified as protective factors. These markers were the most strongly associated with BP among all immunophenotypes tested. In our single-cell sequencing analysis, the low cell count in the peripheral blood of BP patients precluded subgroup analysis of M-MDSCs. However, we analyzed CD16 (FCGR3A) and CD62L (SELL). Results indicated that, compared to healthy controls, the expression of these markers on neutrophils was significantly elevated in BP patients. The expression of CD62L (SELL) in monocytes of BP patients was slightly higher than in healthy controls. Flow cytometry analysis of BP-like mice revealed a significant increase in the proportion of M-MDSCs and a decrease in CD16 levels on CD14−CD16+ monocytes compared to controls.

M-MDSCs are immature myeloid cells with potent immunosuppressive functions, and their expansion is typically associated with chronic inflammation, tumors,[45–47] and autoimmune diseases.[48] Mouse M-MDSCs are characterized as CD11b+Ly6C+Ly6G^{-}, partially overlapping with monocytes.[49,50] In viral infection models, M-MDSCs suppress T cell responses via the iNOS/NO pathway, and subsets with high expression of Ly6C and CD11b have stronger inhibitory

capacity.[51] This study found that an increased number of circulating M-MDSCs is a risk factor for BP. To date, no studies have reported on the mechanisms underlying the role of M-MDSCs in BP. In melanoma patients with immune-related adverse events after immune checkpoint inhibitor treatment, the use of ICIs was found to be associated with an increase in the number of M-MDSCs and a decrease in Treg frequency,[52] indicating that the increase in M-MDSCs to some extent suppresses the number or function of Tregs. Defects in Treg cell function lead to the spontaneous production of IgG autoantibodies against BP230 and type XVII collagen (COL17), and adoptive transfer of CD4+ T cells can induce the production of autoantibodies against full-length COL17 and BP230−1[53,54] However, in periprosthetic joint infection, M-MDSCs increase Treg activity through the CXCL16 - CXCR6 ligand-receptor signaling pathway,[55] demonstrating a positive regulatory effect on Treg function. Therefore, the mechanism of M-MDSCs in BP needs to be interpreted cautiously and cannot be deduced solely based on their role in other diseases. Further functional exploration in the context of BP is required.

CD62L (L-selectin) is a cell adhesion molecule that regulates the recruitment of monocytes from blood to tissues during inflammation,[56] which represents a critical initial step in their migration from blood vessels to inflammatory sites.[57,58] In experimental autoimmune encephalomyelitis mice, CD62L-deficient mice activate autoreactive T cells but do not directly cause central nervous system myelin damage,[59,60] suggesting that CD62L may be involved in recruiting monocyte/macrophage infiltration during the effector phase rather than directly inducing the disease. This study found that reduced expression of CD62L on monocyte surfaces is associated with an increased risk of BP. CD62L enables monocytes to adhere to vascular endothelium and migrate into tissues. The MR results support the hypothesis that during BP onset, inflammatory cells (including monocytes) migrate to affected skin tissue, leading to a decrease in their numbers in the circulating blood. Combined with previous findings regarding CD62L in experimental autoimmune encephalomyelitis, our results align with the pathological feature of extensive monocyte/macrophage infiltration in BP skin lesions. After being recruited to local tissues, monocytes may differentiate into activated macrophages or dendritic cells,[58] presenting autoantigens and secreting pro-inflammatory factors, directly exacerbating inflammation and damage at the basement membrane zone.

To date, monocytes have been extensively studied in the pathogenesis of BP.[61] Monocytes are classified into classical, intermediate, and non-classical subsets; the non-classical subset is defined by low CD14 and high CD16 expression (CD14-/lowCD16+).[62] Functionally, Fc receptors (FcRs) are categorized into two primary classes based on their signaling outcomes. The first class comprises activating FcRs that trigger effector responses in target cells upon ligand binding. These receptors either possess an Immunoreceptor Tyrosine-based Activation Motif (ITAM) directly within their cytoplasmic domains, as seen in FcγRIIA and FcγRIIC, or associate with auxiliary polypeptide chains harboring ITAMs, such as FcεRI, FcγRI, FcαRI, and FcγRIIIA. Structurally, ITAMs are characterized by a conserved YxxL sequence pair separated by 7 to 12 variable amino acids, mirroring the signaling motifs found in T-cell and B-cell antigen receptor complexes. Conversely, the second class includes inhibitory FcRs that fail to induce cellular activation upon ligation. Instead of ITAMs, these receptors contain an Immunoreceptor Tyrosine-based Inhibition Motif (ITIM) within their intracellular regions. Characterized by a V/IxYxxL consensus sequence, ITIMs mediate the suppression of cell activation when co-aggregated with ITAM-bearing receptor complexes.[63,64]

CD16, a type III Fcγ receptor, is associated with dermal-epidermal separation induced by monocytes and neutrophils, leading to increased reactive oxygen species (ROS) production, a process dependent on adhesion and FcγRIII binding. Upon stimulation by the granule-poor fraction of monocyte supernatants, neutrophils increased their release of MMP-9, subsequently degrading the extracellular collagen domain of the recombinant 180-kD BP antigen and cleaving the dermal-epidermal junction (DEJ), thereby promoting blister formation.[61,65,66] When monocytes are co-cultured with neutrophils, they can synergistically release proteases (such as MMP-9), leading to the hydrolysis of BP180 protein and epidermal-dermal separation,[61,67] CD16+ monocytes may enhance immune complex-mediated activation through FcγRIII, promoting this process. Our scRNA-seq analysis show that when suffering from BP, the expression of FCGR3A (CD16) and SELL (CD62L) significantly increased on neutrophils (the HC group only expressed significantly on NK and T cells). This is consistent with the hypothesis that CD16 on monocytes may be involved in the crosstalk between monocytes and neutrophils, potentially contributing to BP pathogenesis, While the in vitro experiments suggest a pathogenic role for CD16 in BP, our MR analysis indicated a negative genetic association between CD16 on CD14-CD16+ monocytes and BP risk (OR=0.83). This apparent discrepancy, together with the minimal FCGR3A expression in monocytes observed in our scRNA-seq data, suggests that the relationship between CD16 and BP is complex and

warrants further investigation. This also supports a hypothesis that CD16 (FcγIII), as a receptor for IgG, is consumed by IgG produced by the body during BP onset through FcγIII ligand-receptor binding, forming immune complexes that deposit in the skin basement membrane zone, thereby reducing its levels in circulation. Adult mouse intestinal epithelial cells also express FcγRII (CD32) and FcγRIII (CD16), with significant upregulation after immune stimulation, and they bind IgG at the basement membrane of the intestinal epithelium. Confocal microscopy revealed co-localization with IgG.[68] Given that the dermal-epidermal junction in BP is similar to the intestinal epithelial-stromal barrier, we speculate that CD16 on monocytes and epidermal structures may be involved in the recognition, retention, and pro-inflammatory activation of IgG autoantibody-immune complexes in the basement membrane zone, thereby promoting blister formation in bullous pemphigoid. The F(ab′)2 fragments of IVIg exhibit strong binding affinity to recombinant FcγIII molecules. Anti-FcγIII F(ab′)2 fragments derived from IVIg exhibit dose-dependent binding, whereas F(ab′)2 components depleted of anti-FcγIII do not bind to FcγIII.[69] In Kawasaki disease, high-dose immunoglobulin therapy inhibited NF-κB activation in human monocytes. Flow cytometry analysis revealed that immunoglobulin therapy significantly reduced the expression of Fcγ receptors on monocytes, but Western blot and quantitative PCR showed no effect on FcγIII protein and mRNA levels, indicating that immunoglobulin only blocks the function of FcγII on monocyte/macrophage membranes.[70] Using flow cytometry, they also assessed the binding of F(ab′)2 fragments to membrane-bound FcγRIII in Jurkat cells transfected with FcγRIII-encoding cDNA. Immunopurified anti-FcγRIII antibodies ultimately confirmed that anti-FcγRIII (CD) antibodies could inhibit immune complex-stimulated receptor-dependent cellular activation by preventing the ability of mouse IgG-sensitized transfected Jurkat cells to form FcγRIII-dependent rosettes with sheep red blood cells.[69] In BP, after immune complex deposition, immune cells are activated, leading to complement activation and the generation of anaphylatoxins such as C3a/C5a, which recruit more neutrophils to the injury site. When neutrophils contact rough titanium surfaces, the release of ROS and NETs increases,[71] promoting the formation of the membrane attack complex (MAC) and directly damaging tissues.[72]

Consequently, targeting CD16 and CD62L on the surface of monocytes represents a promising novel therapeutic approach to impede tissue damage in BP. Our primary distinction from experimental or clinical investigations stems from the fact that all studies have been conducted after the onset of BP, which limits their ability to clarify the causal relationship between BP and immune cells when the temporal sequences remain unclear. A key advantage of MR is its utilization of SNPs as instrumental variables, which helps to alleviate the effects of potential confounding variables and reverse causation. The distribution and migration of monocytes, along with their associations with ethnicity and disease, are highly intricate. Nonetheless, the role of monocytes in BP may be of particular importance, though further studies are needed to establish their precise contributions. However, there are still gaps in our understanding of the epidemiology and monocyte associations concerning BP, which future research should aim to fill.

We acknowledge that our study has several limitations. Given that BP is a rare disease, this GWAS included only 219 cases, resulting in a limited sample size, making the reliable detection of weak-to-moderate genetic effects (OR < 1.3) challenging. Some extreme SNPs can interfere with MR analysis, and residual pleiotropic bias remains even after correction. Therefore, this study only considers phenotypes with FDR-corrected $q < 0.05$ as reliable genetic signals; however, null results do not rule out potential associations. MR can only suggest genetic correlations but cannot confirm true biological causality; it is difficult to distinguish between immune cell abundance and surface marker expression, nor can it determine whether immune changes are the cause of BP onset or secondary inflammatory damage. The positive MR signals were observed exclusively in monocytes, whereas peripheral blood scRNA-seq revealed more significant transcriptional differences in neutrophils and dendritic cells. The expression of CD16 and CD62L in peripheral monocytes of patients is not statistically significant. This discrepancy arises because MR reflects pre-onset innate susceptibility traits, while sequencing samples are taken from diagnosed patients, where extensive monocyte migration to skin lesions results in low peripheral expression. Additionally, this study lacks single-cell data from skin lesions. Furthermore, the single-cell analysis uses only a single public dataset without external validation from an independent patient cohort. There are species differences between our animal models and human diseases, and our flow cytometry validation evidence can only serve as auxiliary support. The pathogenic pathways related to CD16, CD62L, and M-MDSC mentioned in the text are all inferred hypotheses, lacking direct evidence from human tissues and in vitro functional experiments, and still require subsequent functional studies for validation.

Conclusion

To the best of our knowledge, this study represents the inaugural effort to investigate the causal relationship between BP and immune cells by integrating MR analysis with scRNA-seq analysis, and an animal model was used for verification. Our findings suggest genetic associations between various immunophenotypes and BP, highlighting immunophenotypes that warrant further mechanistic investigation, highlighting the complex interplay between the immune system and the pathogenesis of BP. The absolute count of M-MDSCs showed a positive genetic association with BP risk, whereas CD62L expression on monocytes and CD16 on CD14-CD16+ monocytes showed inverse genetic associations. Genes associated with these immunophenotypes were enriched in immune-related processes, including RNA splicing, the positive regulation of cytokine production, signaling pathways that modulate immune responses, and the differentiation of mononuclear cells. Importantly, MR analysis helps mitigate confounding factors inherent in observational studies. This study paves the way for further exploration of the biological mechanisms underlying BP, potentially facilitating earlier interventions and therapeutic approaches. The results of our investigation enhance current understanding of immune cell participation in BP, providing insights that could inform strategies for BP prevention.

Data Sharing Statement

The data used to generate the results in this study were obtained from genome-wide association study summary statistics, which were publicly released by genetic consortia.

Ethics Approval and Consent to Participate

This study was carried out in accordance with the relevant guidelines. All animal experiments were approved by the Animal Ethics Committee of Yunnan Minzu University (approval number: YMU-AFEC-2023-A020), It refers to the "Guidelines for Ethical Review of Laboratory Animal Welfare (GB/T 35892-2018)" issued by China in 2018. All human genetic data analyzed in this study were fully de-identified, publicly available summary statistics downloaded from open-access GWAS databases. No individual identifiable information or human biosamples were involved, and no human interventions were performed. This research meets the exemption criteria specified in Article 32 Items 1 and 2 of the Measures for Ethical Review of Life Science and Medical Research Involving Human Subjects issued by China on February 18, 2023; therefore, formal institutional ethical review approval is not required.

Acknowledgments

We thank all consortium studies for publicly making the summary association statistics data available. We thank all the reviewers for their comments and contributions to this manuscript. We would like to thank the Pharmacology Laboratory of Yunnan Minzu University for providing the experimental facilities.

Author Contributions

All authors made a significant contribution to the work reported, whether that is in the conception, study design, execution, acquisition of data, analysis and interpretation, or in all these areas; took part in drafting, revising or critically reviewing the article; gave final approval of the version to be published; have agreed on the journal to which the article has been submitted; and agree to be accountable for all aspects of the work.

Funding

This study was supported by National Natural Science Foundation of China(82260940) to Jianzhou Ye; The Engineering Research Center of Traditional Chinese Medicine for the Treatment of Skin Diseases of the Department of Education of Yunnan Province (2022(J)10-A05-03) and The Key project of science and technology plan of Yunnan Provincial Department of Science and Technology (202501AS070158) to Xuesong Yang. The Yunnan Science and Technology Talent and Platform Program(202105AG070012)to Zhimin Wang.

Disclosure

The authors report no conflicts of interest in this work.

References

1. Persson MSM, Begum N, Grainge MJ, Harman KE, Grindlay D, Gran S. The global incidence of bullous pemphigoid: a systematic review and meta-analysis. *Br J Dermatol*. 2022;186(3):414–425. doi:10.1111/bjd.20743
2. Schinner J, Cunha T, Mayer JU, et al. Skin-infiltrating T cells display distinct inflammatory signatures in lichen planus, bullous pemphigoid and pemphigus vulgaris. *Front Immunol*. 2023;14:1203776. doi:10.3389/fimmu.2023.1203776
3. Berkani N, Joly P, Golinski ML, et al. Author correction: b-cell depletion induces a shift in self antigen specific B-cell repertoire and cytokine pattern in patients with bullous pemphigoid. *Sci Rep*. 2019;9(1):18991. doi:10.1038/s41598-019-54421-6
4. Yan T, Xie Y, Liu Y, et al. Dupilumab effectively and rapidly treats bullous pemphigoid by inhibiting the activities of multiple cell types. *Front Immunol*. 2023;14:1194088. doi:10.3389/fimmu.2023.1194088
5. Fang H, Zhang Y, Li N, Wang G, Liu Z. The autoimmune skin disease bullous pemphigoid: the role of mast cells in autoantibody-induced tissue injury. *Front Immunol*. 2018;9:407. doi:10.3389/fimmu.2018.00407
6. Fang H, Shao S, Xue K, et al. Neutrophil extracellular traps contribute to immune dysregulation in bullous pemphigoid via inducing B-cell differentiation and antibody production. *FASEB J*. 2021;35(7):e21746. doi:10.1096/fj.202100145R
7. Li SZ, Jin XX, Ge XL, Zuo YG, Jin HZ. Thymic stromal lymphopoietin is implicated in the pathogenesis of bullous pemphigoid by dendritic cells. *J Immunol Res*. 2020;2020:4594630. doi:10.1155/2020/4594630
8. Delli FS, Sotiriou E, Lazaridou E, et al. Total IgE, eosinophils, and interleukins 16, 17A, and 23 correlations in severe bullous pemphigoid and treatment implications. *Dermatologic Therapy*. 2020;33(6):e13958. doi:10.1111/dth.13958
9. Ujiie H, Yoshimoto N, Natsuga K, et al. Immune reaction to type XVII collagen induces intramolecular and intermolecular epitope spreading in experimental bullous pemphigoid models. *Front Immunol*. 2019;10:1410. doi:10.3389/fimmu.2019.01410
10. Davey Smith G, Hemani G. Mendelian randomization: genetic anchors for causal inference in epidemiological studies. *Hum Mol Gen*. 2014;23 (R1):R89–98. doi:10.1093/hmg/ddu328
11. Kolodziejczyk AA, Kim JK, Svensson V, Marioni JC, Teichmann SA. The technology and biology of single-cell RNA sequencing. *Molecular Cell*. 2015;58(4):610–620. doi:10.1016/j.molcel.2015.04.005
12. Vetter TR, Mascha EJ. Bias, confounding, and interaction: lions and tigers, and bears, oh my! *Anesthesia Analg*. 2017;125(3):1042–1048. doi:10.1213/ANE.0000000000002332
13. Peto R, Collins R. Randomization. *Nature*. 1994;372(6507):588. doi:10.1038/372588d0
14. Orrù V, Steri M, Sidore C, et al. Complex genetic signatures in immune cells underlie autoimmunity and inform therapy. *Nature Genet*. 2020;52 (10):1036–1045. doi:10.1038/s41588-020-0684-4
15. Liu T, Wang Z, Xue X, et al. Single-cell transcriptomics analysis of bullous pemphigoid unveils immune-stromal crosstalk in type 2 inflammatory disease. *Nat Commun*. 2024;15(1):5949. doi:10.1038/s41467-024-50283-3
16. Cai J, Li X, Wu S, et al. Assessing the causal association between human blood metabolites and the risk of epilepsy. *J Transl Med*. 2022;20(1):437. doi:10.1186/s12967-022-03648-5
17. Bowden J, Davey Smith G, Burgess S. Mendelian randomization with invalid instruments: effect estimation and bias detection through egger regression. *Int J Epidemiol*. 2015;44(2):512–525. doi:10.1093/ije/dyv080
18. Burgess S, Bowden J, Fall T, Ingelsson E, Thompson SG. Sensitivity analyses for robust causal inference from mendelian randomization analyses with multiple genetic variants. *Epidemiology*. 2017;28(1):30–42. doi:10.1097/EDE.0000000000000559
19. Bowden J, Del Greco MF, Minelli C, Davey Smith G, Sheehan N, Thompson J. A framework for the investigation of pleiotropy in two-sample summary data mendelian randomization. *Stat Med*. 2017;36(11):1783–1802. doi:10.1002/sim.7221
20. Burgess S, Thompson SG. Interpreting findings from mendelian randomization using the MR-egger method. *Eur j epidemiol*. 2017;32(5):377–389. doi:10.1007/s10654-017-0255-x
21. Bowden J, Spiller W, Del Greco MF, et al. Improving the visualization, interpretation and analysis of two-sample summary data mendelian randomization via the radial plot and radial regression. *Int J Epidemiol*. 2018;47(4):1264–1278. doi:10.1093/ije/dyy101
22. Verbanck M, Chen CY, Neale B, Do R. Detection of widespread horizontal pleiotropy in causal relationships inferred from mendelian randomization between complex traits and diseases. *Nature Genet*. 2018;50(5):693–698. doi:10.1038/s41588-018-0099-7
23. Stuart T, Butler A, Hoffman P, et al. Comprehensive integration of single-cell data. *Cell*. 2019;177(7):1888–1902.e1821. doi:10.1016/j.cell.2019.05.031
24. Qiu X, Hill A, Packer J, Lin D, Ma YA, Trapnell C. Single-cell mRNA quantification and differential analysis with Census. *Nature Methods*. 2017;14(3):309–315. doi:10.1038/nmeth.4150
25. González-Blas C B, De Winter S, Hulselmans G, et al. SCENIC+: single-cell multiomic inference of enhancers and gene regulatory networks. *Nature Methods*. 2023;20(9):1355–1367. doi:10.1038/s41592-023-01938-4
26. Kanehisa M, Goto S. KEGG: kyoto encyclopedia of genes and genomes. *Nucleic Acids Res*. 2000;28(1):27–30. doi:10.1093/nar/28.1.27
27. Su Z, Huang Y, Gu X. Tissue-driven hypothesis with Gene Ontology (GO) analysis. *Ann Biomed Eng*. 2007;35(6):1088–1094. doi:10.1007/s10439-007-9269-y
28. Akbarialiabad H, Schmidt E, Patsatsi A, et al. Bullous pemphigoid. *Nat Rev Dis Primers*. 2025;11(1):12. doi:10.1038/s41572-025-00595-5
29. Delgado JC, Turbay D, Yunis EJ, et al. A common major histocompatibility complex class II allele HLA-DQB1* 0301 is present in clinical variants of pemphigoid. *Proc Natl Acad Sci USA*. 1996;93(16):8569–8571. doi:10.1073/pnas.93.16.8569
30. Lo Schiavo A, Ruocco E, Brancaccio G, Caccavale S, Ruocco V, Wolf R. Bullous pemphigoid: etiology, pathogenesis, and inducing factors: facts and controversies. *Clin Dermatol*. 2013;31(4):391–399. doi:10.1016/j.clindermatol.2013.01.006
31. Arakawa M, Dainichi T, Ishii N, et al. Lesional Th17 cells and regulatory T cells in bullous pemphigoid. *Exp Dermatol*. 2011;20(12):1022–1024. doi:10.1111/j.1600-0625.2011.01378.x
32. Hashimoto T, Takahashi H, Sakaguchi S. Regulatory T-cell deficiency and autoimmune skin disease: beyond the scurfy mouse and immune dysregulation, polyendocrinopathy, enteropathy, X-linked syndrome. *J Allergy Clin Immunol*. 2018;142(6):1754–1756. doi:10.1016/j.jaci.2018.08.028
33. Liu Y, Wang H, Taylor M, et al. Classification of human chronic inflammatory skin disease based on single-cell immune profiling. *Sci Immunol*. 2022;7(70):eabl9165. doi:10.1126/sciimmunol.abl9165

34. Ujiie H. What's new in the pathogeneses and triggering factors of bullous pemphigoid. *J Dermatol*. 2023;50(2):140–149. doi:10.1111/1346-8138.16654
35. Lytvyn Y, Rahat S, Mufti A, et al. Biologic treatment outcomes in mucous membrane pemphigoid: a systematic review. *J Am Acad Dermatol*. 2022;87(1):110–120. doi:10.1016/j.jaad.2020.12.056
36. Kennedy A, Waters E, Rowshanravan B, et al. Differences in CD80 and CD86 transendocytosis reveal CD86 as a key target for CTLA-4 immune regulation. *Nat Immunol*. 2022;23(9):1365–1378. doi:10.1038/s41590-022-01289-w
37. Shalata W, Weissmann S, Itzhaki Gabay S, et al. A retrospective, single-institution experience of bullous pemphigoid as an adverse effect of immune checkpoint inhibitors. *Cancers*. 2022;14(21):5451. doi:10.3390/cancers14215451
38. Huang Y, Zheng H, Zhu Y, et al. Loss of CD28 expression associates with severe T-cell exhaustion in acute myeloid leukemia. *Front Immunol*. 2023;14:1139517. doi:10.3389/fimmu.2023.1139517
39. Wang CJ, Heuts F, Ovcinnikovs V, et al. CTLA-4 controls follicular helper T-cell differentiation by regulating the strength of CD28 engagement. *Proc Natl Acad Sci USA*. 2015;112(2):524–529. doi:10.1073/pnas.1414576112
40. Bluestone JA, St Clair EW, Turka LA. CTLA4Ig: bridging the basic immunology with clinical application. *Immunity*. 2006;24(3):233–238. doi:10.1016/j.immuni.2006.03.001
41. Okazaki A, Miyagawa S, Yamashina Y, Kitamura W, Shirai T. Polymorphisms of HLA-DR and -DQ genes in Japanese patients with bullous pemphigoid. *J Dermatol*. 2000;27(3):149–156. doi:10.1111/j.1346-8138.2000.tb02141.x
42. Seignalet J, Guillot B, Guilhou JJ, Meynadier J. Probable association of HLA-DR5 with bullous pemphigoid. *Revue francaise de transfusion et immuno-hematologie*. 1988;31(1):11–18. doi:10.1016/S0338-4535(88)80063-1
43. László S, Neumann S, Hertl M, Hunzelmann N. Generation of increased numbers of HLA-DR(high) IgG+ plasma cells in the peripheral blood of patients with bullous pemphigoid: NC16a-specific cells belong to the short-lived plasma blast population. *J invest Dermatol*. 2010;130(12):2838–2841. doi:10.1038/jid.2010.213
44. Gao XH, Winsey S, Li G, et al. HLA-DR and DQ polymorphisms in bullous pemphigoid from northern China. *Clin Exp Dermatol*. 2002;27(4):319–321. doi:10.1046/j.1365-2230.2002.01037.x
45. Takacs GP, Kreiger CJ, Luo D, et al. Glioma-derived CCL2 and CCL7 mediate migration of immune suppressive CCR2(+)/CX3CR1(+) M-MDSCs into the tumor microenvironment in a redundant manner. *Front Immunol*. 2022;13:993444. doi:10.3389/fimmu.2022.993444
46. Takacs GP, Garcia JS, Hodges CA, Kreiger CJ, Sherman A, Harrison JK. CSF1R ligands expressed by murine gliomas promote M-MDSCs to suppress CD8(+) T cells in a NOS-dependent manner. *Cancers*. 2024;16(17):3055. doi:10.3390/cancers16173055
47. Takacs GP, Garcia JS, Hodges CA, Kreiger CJ, Sherman A, Harrison JK. Glioma-derived M-CSF and IL-34 license M-MDSCs to suppress CD8(+) T cells in a NOS-dependent manner. *bioRxiv*. 2024.
48. Deng J, Tan S, Liu R, et al. Chinese medicine formula PSORI-CM02 alleviates psoriatic dermatitis via M-MDSCs and Th17 crosstalk. *Front Pharmacol*. 2020;11:563433. doi:10.3389/fphar.2020.563433
49. Zou Y, Kamada N, Seong SY, Seo SU. CD115(-) monocytic myeloid-derived suppressor cells are precursors of OLFM4(high) polymorphonuclear myeloid-derived suppressor cells. *Commun Biol*. 2023;6(1):272. doi:10.1038/s42003-023-04650-3
50. Zhao Y, Wu T, Shao S, Shi B, Zhao Y. Phenotype, development, and biological function of myeloid-derived suppressor cells. *Oncoimmunology*. 2016;5(2):e1004983. doi:10.1080/2162402X.2015.1004983
51. O'Connor MA, Fu WW, Green KA, Green WR. Subpopulations of M-MDSCs from mice infected by an immunodeficiency-causing retrovirus and their differential suppression of T- vs B-cell responses. *Virology*. 2015;485:263–273. doi:10.1016/j.virol.2015.07.020
52. Lepper A, Bitsch R, Ozbay Kurt FG, et al. Melanoma patients with immune-related adverse events after immune checkpoint inhibitors are characterized by a distinct immunological phenotype of circulating T cells and M-MDSCs. *Oncoimmunology*. 2023;12(1):2247303. doi:10.1080/2162402X.2023.2247303
53. Muramatsu K, Ujiie H, Kobayashi I, et al. Regulatory T-cell dysfunction induces autoantibodies to bullous pemphigoid antigens in mice and human subjects. *J Allergy Clin Immunol*. 2018;142(6):1818–1830e1816. doi:10.1016/j.jaci.2018.03.014
54. Haeberle S, Wei X, Bieber K, et al. Regulatory T-cell deficiency leads to pathogenic bullous pemphigoid antigen 230 autoantibody and autoimmune bullous disease. *J Allergy Clin Immunol*. 2018;142(6):1831–1842e1837. doi:10.1016/j.jaci.2018.04.006
55. Wu X, Pan B, Chu C, et al. CXCL16/CXCR6/TGF-beta feedback loop between M-MDSCs and treg inhibits anti-bacterial immunity during biofilm infection. *Adv Sci*. 2025;12(7):e2409537. doi:10.1002/advs.202409537
56. Adams DH, Shaw S. Leucocyte-endothelial interactions and regulation of leucocyte migration. *Lancet*. 1994;343(8901):831–836. doi:10.1016/S0140-6736(94)92029-X
57. Rutkowska E, Kwiecien I, Klos K, Rzepecki P, Chcialowski A. Intermediate monocytes with PD-L1 and CD62L expression as a possible player in active SARS-CoV-2 infection. *Viruses*. 2022;14(4):819. doi:10.3390/v14040819
58. Lu J, Lv S, Pang J, et al. M2c macrophages protect mice from adriamycin-induced nephropathy by upregulating CD62L in tregs. *Mediators Inflamm*. 2022;2022:1153300. doi:10.1155/2022/1153300
59. Grewal IS, Foellmer HG, Grewal KD, et al. CD62L is required on effector cells for local interactions in the CNS to cause myelin damage in experimental allergic encephalomyelitis. *Immunity*. 2001;14(3):291–302. doi:10.1016/S1074-7613(01)00110-8
60. Li O, Liu JQ, Zhang H, Zheng P, Liu Y, Bai XF. CD62L is required for the priming of encephalitogenic T cells but does not play a major role in the effector phase of experimental autoimmune encephalomyelitis. *Scand J Immunol*. 2006;64(2):117–124. doi:10.1111/j.1365-3083.2006.01783.x
61. de Graauw E, Sitaru C, Horn MP, et al. Monocytes enhance neutrophil-induced blister formation in an ex vivo model of bullous pemphigoid. *Allergy*. 2018;73(5):1119–1130. doi:10.1111/all.13376
62. Wong KL, Tai JJ, Wong WC, et al. Gene expression profiling reveals the defining features of the classical, intermediate, and nonclassical human monocyte subsets. *Blood*. 2011;118(5):e16–31. doi:10.1182/blood-2010-12-326355
63. Nimmerjahn F, Ravetch JV. FcgammaRs in health and disease. *Curr Top Microbiol Immunol*. 2011;350:105–125. doi:10.1007/82_2010_86
64. Ravetch JV, Bolland S. IgG Fc receptors. *Annu Rev Immunol*. 2001;19:275–290. doi:10.1146/annurev.immunol.19.1.275
65. Ståhle-Bäckdahl M, Inoue M, Guidice GJ, Parks WC. 92-kD gelatinase is produced by eosinophils at the site of blister formation in bullous pemphigoid and cleaves the extracellular domain of recombinant 180-kD bullous pemphigoid autoantigen. *J Clin Invest*. 1994;93(5):2022–2030. doi:10.1172/JCI117196

66. Riani M, Le Jan S, Plée J, et al. Bullous pemphigoid outcome is associated with CXCL10-induced matrix metalloproteinase 9 secretion from monocytes and neutrophils but not lymphocytes. *J allergy Clin Immunol*. 2017;139(3):863–872.e863. doi:10.1016/j.jaci.2016.08.012
67. Mizuno Y, Shibata S, Ito Y, et al. Interleukin-26-DNA complexes promote inflammation and dermal-epidermal separation in a modified human cryosection model of bullous pemphigoid. *Front Immunol*. 2022;13:1013382. doi:10.3389/fimmu.2022.1013382
68. Moreno-Fierros L, Verdin-Teran SL, Garcia-Hernandez AL. Intraperitoneal Immunization with Cry1Ac protoxin from bacillus thuringiensis provokes upregulation of Fc-gamma-II/and Fc-gamma-III receptors associated with IgG in the intestinal epithelium of mice. *Scand J Immunol*. 2015;82(1):35–47. doi:10.1111/sji.12305
69. Bouhlal H, Martinvalet D, Teillaud JL, et al. Natural autoantibodies to Fcgamma receptors in intravenous immunoglobulins. *J Clin Immunol*. 2014;34 (Suppl 1):S4–11.
70. Ichiyama T, Ueno Y, Hasegawa M, Niimi A, Matsubara T, Furukawa S. Intravenous immunoglobulin inhibits NF-kappaB activation and affects Fcgamma receptor expression in monocytes/macrophages. *Naunyn Schmiedebergs Arch Pharmacol*. 2004;369(4):428–433. doi:10.1007/s00210-004-0877-x
71. Elangovan G, Mello-Neto JM, Tadakamadla SK, Reher P, Figueredo CMS. A systematic review on neutrophils interactions with titanium and zirconia surfaces: evidence from in vitro studies. *Clin Exp Dent Res*. 2022;8(4):950–958. doi:10.1002/cre2.582
72. Aredo B, Zhang K, Chen X, Wang CX, Li T, Ufret-Vincenty RL. Differences in the distribution, phenotype and gene expression of subretinal microglia/macrophages in C57BL/6N (Crb1 rd8/rd8) versus C57BL6/J (Crb1 wt/wt) mice. *J Neuroinflammation*. 2015;12:6. doi:10.1186/s12974-014-0221-4

Clinical, Cosmetic and Investigational Dermatology

Dovepress
Taylor & Francis Group

Publish your work in this journal

Clinical, Cosmetic and Investigational Dermatology is an international, peer-reviewed, open access, online journal that focuses on the latest clinical and experimental research in all aspects of skin disease and cosmetic interventions. This journal is indexed on CAS. The manuscript management system is completely online and includes a very quick and fair peer-review system, which is all easy to use. Visit http://www.dovepress.com/testimonials.php to read real quotes from published authors.

Submit your manuscript here: https://www.dovepress.com/clinical-cosmetic-and-investigational-dermatology-journal